DOE-ET-53088-128 IFSR #128

FREE-BOUNDARY STABILITY OF STRAIGHT STELLARATORS

D. C. Barnes
John R. Cary
Institute for Fusion Studies
The University of Texas at Austin

February 1984

Free-Boundary Stability of Straight Stellarators

D. C. Barnes and John R. Cary

Institute for Fusion Studies

University of Texas

Austin, Texas 78712

ABSTRACT

The sharp-boundary model is used to investigate the stability of straight stellarators to free-boundary, long-wavelength modes. To correctly analyze the heliac configuration, previous theory is generalized to the case of arbitrary helical aspect ratio (ratio of plasma radius to periodicity length). A simple low-β criterion involving the vacuum field and the normalized axial current is derived and used to investigate a large variety of configurations. The predictions of this low-β theory are verified by numerical minimization of δW at arbitrary β. The heliac configuration is found to be remarkably stable, with a critical β of over 15% determined by the lack of equilibrium rather than the onset of instability. In addition, other previously studied systems are found to be stabilized by net axial plasma current.

I. Introduction

Recently it has been proposed[1] that an $\ell = 1$ (ℓ being the poloidal mode number of the dominant helical field) stellarator with a helical plasma surrounding a central, current-carrying conductor (herein known as a heliac) would have good stability properties. This has been confirmed[2] for the short-wavelength, fixed-boundary modes of straight (non-toroidal) heliacs. The present work is directed toward determining the stability of straight heliacs to long-wavelength, free-boundary modes. This is especially important in light of past theoretical and experimental work on the $\ell = 1$ Scyllac,[3] in which the stability of free-boundary modes placed the critical restriction on high-β plasma operation.

The previous Scyllac stability results depended on three parameters: β, the relative plasma pressure; δ, the relative deviation of the plasma boundary from circular; and $\varepsilon \equiv ha$, the product of the plasma radius and the equilibrium helical pitch number ($h = 2\pi/L$, where L is the length of a helical period). Results obtained by expanding in either δ or ε but keeping β of order unity found[3] that the free-boundary mode with $k = 0$ (the helical wavenumber) and $m = 1$ (the poloidal modenumber) was strongly unstable for $\ell \neq 1$ and weakly unstable for $\ell = 1$. In the latter case, the mode could be stabilized by wall effects. Other work[4] showed that for $\ell \geq 2$ this mode could be stable for smaller β. However, later work[5,6] found that these systems were unstable to a long-wavelength, free-boundary, interchange-like mode with $k \neq 0$ for any positive value of β. In concert, these results indicate the need for determining the stability of these modes in the heliac configuration.

All of the above conclusions were obtained by modeling the confined plasma as a sharp-boundary system in which the plasma pressure is constant inside a given flux surface and vanishes outside this surface. Later calculations, in which the plasma was modeled by a diffuse profile equilibrium, reproduced the above features with only quantitative modifications.

Motivated by these previous studies, the two-dimensional straight heliac is modeled as a sharp-boundary system. Because the growth rates of unstable modes are expected to be sensitively dependent on the helical curvature, the present analysis generalizes previous work by allowing for arbitrary ε. A sharp-boundary equilibrium is computed for an arbitrarily shaped plasma by solving a potential problem for the interior domain to determine the interior vacuum field. Then pressure balance gives the exterior surface field.

Stability is investigated in the usual way[7] by minimizing δW. The plasma and vacuum contributions to δW may be minimized holding the normal surface displacement fixed. The minima are given in terms of the solutions of interior and exterior potential problems. Linear stability is then determined by minimizing the resulting δW with respect to the surface displacement.

A low-β analysis provides a deeper understanding of the previously found[5,6] surface interchange instability. When the plasma pressure vanishes, a marginally stable mode exists. With the introduction of plasma pressure and current, this mode can be either stabilized or destabilized. If the net plasma current vanishes, the stability of this mode is given by the usual V'' criterion.[8,9] However, in general there is a contribution from the interaction of a small axial current

with the vacuum shear, which is stabilizing for the proper choice of current. This means that the $\ell = 2$ and $\ell = 3$ stellarators, which were previously found to be unstable, can be stabilized by a net axial current.

Still, there is a preference for systems without net axial current, which can more easily be made to operate in steady state. According to the present results, such systems must have a vacuum magnetic well. Within the set of helical symmetric systems, this is, in fact, a property of only the heliac system and a few other systems with helical magnetic axes.[10,11] Thus, the requirement of low-β stability to free-boundary modes leads to these systems alone.

To determine the limiting value of β, it is necessary to extend the low-β theory to arbitrary β. This requires an efficient and accurate numerical solution to the potential problem. In the present work, a Fourier expansion technique similar to that of Ref. 6 is used. However, here the exact free-space helical Green's function[12] is used.

The results of the high-β theory are quite optimistic. In the case of the heliac configuration, the limiting β-value is due to loss of equilibrium rather than the existence of instabilities. This occurs at a β-value of over 15%. Relatively large critical-β values are also found for sharp-boundary stellarators stabilized by net current.

The remainder of this paper is organized as follows. In Sec. II, the general formulation of the problem is given. After the geometry is described and appropriate coordinates are introduced, the sharp-boundary equilibrium problem is formulated. Then δW is minimized with respect to the plasma and vacuum perturbed magnetic fields. Sec. III develops the low-β limit of the equilibrium and stability

problems. The criterion for stability at small β is derived and applied to a number of configurations. In Sec. IV, the numerical procedure for solution of the equilibrium and stability problems at arbitrary β is developed and applied to the heliac and to the stabilization of systems with non-zero net axial current. Conclusions are given in Section V.

II. Sharp-Boundary Equilibrium and Stability

The first step in applying the sharp-boundary model is the specification of the bounding surface of the plasma. In the present case, helical symmetry is assumed. This means that unperturbed quantities depend only on the radius r and the helical angle $\varphi \equiv \vartheta - hz$, where (r,ϑ,z) are the usual cylindrical coordinates. Thus, the bounding surface of the plasma can be specified by two functions, $r_s(t)$ and $\varphi_s(t)$, such that the surface is the two parameter family of points,

$$\underset{\sim}{r}_s = r_s(t) \cos [\varphi_s(t) + h\zeta] \hat{x} + r_s(t) \sin [\varphi_s(t) + h\zeta] \hat{y} + \zeta \hat{z} , \quad (1)$$

where $0 \leq t < 2\pi$, and $-\infty < \zeta < \infty$. The parameter t is specified by requiring the surface area element to be constant.

$$\left| \frac{\partial \underset{\sim}{r}_s}{\partial t} \times \frac{\partial \underset{\sim}{r}_s}{\partial \zeta} \right| = \left[(1+h^2 r_s^2) \dot{r}_s^2 + r_s^2 \dot{\varphi}_s^2 \right]^{1/2} = A . \quad (2)$$

The overdot in Eq. (2) denotes differentiation with respect to t. The process of determining t and A given an arbitrary parameterization is discussed in App. A.

A complete coordinate system is defined in the neighborhood of the surface by introducing a normal coordinate η. It is convenient to choose η to measure the normal distance from the surface (see Fig. 1). Thus, the cartesian vector is given by

$$\underset{\sim}{r} = \underset{\sim}{r}_s(t,\zeta) + \eta \hat{n}(t,\zeta) , \quad (3)$$

for small η, where $\hat{n}$ is the unit surface normal

$$\hat{n}(t,\zeta) = A^{-1}\left(r_s\dot{\varphi}_s\,\hat{r} - \dot{r}_s\,\hat{\vartheta} + hr_s\dot{r}_s\,\hat{z}\right) , \tag{4}$$

One should note that Eq. (3) implies that z and ζ are no longer identical off the surface.

The metric tensor for this coordinate system is expressed in terms of the functions $r_s(t)$ and $\varphi_s(t)$ in App. A.

B. Equilibrium

In the sharp-boundary model, plasma currents needed for confining the plasma pressure exist only at the plasma boundary. Thus, the interior and exterior magnetic fields can both be written as gradients of scalar potentials. The interior and exterior solutions must match at the boundary by having the jump in magnetic pressure oppose the jump in plasma pressure.

1. Interior solution

The interior field has the form

$$\underset{\sim}{B}_I = \alpha\nabla(z+\Phi) , \tag{5}$$

where Φ is a single valued potential independent of z and α is a constant whose value is determined by matching to the exterior field. By choice, the value of α is unity when the pressure gradient vanishes. Thus, the vacuum field is

$$\underset{\sim}{B}_0 = \nabla(z+\Phi) . \tag{6}$$

The interior potential Φ is determined by the conditions $\nabla \cdot \underset{\sim}{B}_I = 0$ in the interior plasma region, and $\hat{n} \cdot \underset{\sim}{B}_I = 0$ at the plasma surface. This gives a Neumann potential problem for determining Φ:

$$\nabla^2 \phi = 0 \quad , \tag{7a}$$

with

$$\hat{n} \cdot \nabla \phi = -\hat{n} \cdot \hat{z} = -A^{-1} h r_s \, \hat{r}_s \tag{7b}$$

on the plasma surface. The solution for Φ is found using the free-space Green's function as described in Sec. IV and App. D.

2. Exterior solution

The exterior field similarly may be written as

$$\underset{\sim}{B}_E = \nabla(z + \gamma t + \psi) \quad , \tag{8}$$

where ψ is a single-valued potential independent of z, and γ is a constant. Note that the unit of magnetic field has been chosen to be the exterior axial field strength far from the plasma, by choosing unity as the coefficient of z in Eq. (8). The secular term γt is included in Eq. (8) to allow for nonzero net axial current on the plasma surface. From Ampere's law (in rationalized units) the net axial current is given by

$$I = \oint \underset{\sim}{B}_E \cdot d\underset{\sim}{\ell} = \int_0^{2\pi} dt \; \underset{\sim}{B}_E \cdot \frac{\partial \underset{\sim}{r}}{\partial t} = 2\pi\gamma \; . \tag{9}$$

The constants γ and α and the value of the exterior potential ψ at the plasma surface are determined by pressure balance

$$\frac{1}{2} B_E^2 = \frac{1}{2} B_I^2 + \frac{1}{2} \beta \quad , \tag{10}$$

where β is the ratio of plasma pressure to external axial field pressure. From Eqs. (5) and (8), the covariant components of the magnetic field are,

$$B_{It} = \alpha \frac{\partial \phi}{\partial t} \quad , \qquad B_{I\zeta} = \alpha \quad , \tag{11a}$$

$$B_{Et} = \gamma + \frac{\partial \psi}{\partial t} \quad , \qquad B_{E\zeta} = 1 \quad , \tag{11b}$$

on the plasma surface. Equations (10) and (11) lead to a quadratic equation for B_{Et},

$$g^{tt} B_{Et}^2 + 2 g^{t\zeta} B_{Et} + g^{\zeta\zeta} = \alpha^2 B_0^2 + \beta \quad , \tag{12}$$

which is readily solved for B_{Et}:

$$B_{Et} = - \{ g^{t\zeta} + [(\beta + \alpha^2 B_0^2) g^{tt} - A^{-2}]^{1/2} \} / g^{tt} \quad . \tag{13}$$

The choice of sign in Eq. (13) is such that $\psi = \phi$ when $\gamma, \beta \to 0$ and $\alpha \to 1$. Finally, a relation between α, γ, and the axial current I is obtained by integration of Eq. (13) with respect to t:

$$I = 2\pi\gamma$$
$$= -\int_0^{2\pi} dt \left\{ g^{t\zeta} + \left[(\beta+\alpha^2 B_0^2) g^{tt} - A^{-2} \right]^{1/2} \right\} / g^{tt} \quad . \tag{14}$$

The equilibrium for a particular boundary is, thus, completely specified by the parameters β and I. It is given by the following sequence of operations. First, Eq. (7) is solved to obtain Φ and, hence, $\underset{\sim}{B}_0$. Then, α is found by solving Eq. (14). Of course, a solution for α may not exist if one is attempting to exceed the equilibrium β-limit. Finally, Eq. (13) yields the remaining unknown component of $\underset{\sim}{B}_E$.

C. Stability

Ideal magnetohydrodynamic stability is examined by minimizing δW with a suitable normalization.[7] Minimization of δW with respect to the parallel plasma displacement results in the incompressibility condition $\nabla \cdot \underset{\sim}{\xi} = 0$. Under this condition, δW may be written as

$$\delta W = \delta W_P + \delta W_V + \delta W_S \quad , \tag{15}$$

where the plasma, vacuum, and surface contributions are given by

$$\delta W_P = \frac{1}{2} \int d\underset{\sim}{r} |\underset{\sim}{b}_I|^2 \quad , \tag{16a}$$

$$\delta W_V = \frac{1}{2} \int d\underset{\sim}{r} |\underset{\sim}{b}_E|^2 \quad , \tag{16b}$$

$$\delta W_S = \frac{1}{2} \int dA |\xi|^2 \, \hat{n} \cdot \nabla \frac{1}{2} (B_E^2 - B_I^2) \quad , \tag{16c}$$

where the integrals are over the plasma region, the vacuum region, and

the plasma surface, respectively; $\underset{\sim}{b}_I$ and $\underset{\sim}{b}_E$ are the interior and exterior field perturbations; and ξ is the normal displacement of the plasma surface.

In the sharp-boundary model, δW can be expressed in terms of ξ alone. The dependence of δW_s on ξ is quite explicit. We now show how δW_p and δW_v can be written in terms of ξ.

The plasma and vacuum contributions, δW_P and δW_V are minimized subject to $\nabla \cdot \underset{\sim}{b}_I = 0 = \nabla \cdot \underset{\sim}{b}_E$. The resulting Euler equations are $\nabla \times \underset{\sim}{b}_I = 0 = \nabla \times \underset{\sim}{b}_E$, so that the perturbed fields may be expressed in terms of potentials, $\underset{\sim}{b}_I = \nabla u_I$ and $\underset{\sim}{b}_E = \nabla u_E$. With no conducting wall present, u_E is required to be regular at ∞. Then the minimized δW_P and δW_V are given by (a unit length in ζ is chosen here and in the sequel)

$$\delta W_P = \frac{A}{2} \int_0^{2\pi} dt \; u_I \; \hat{n} \cdot \nabla u_I \; , \tag{17a}$$

and

$$\delta W_V = - \frac{A}{2} \int_0^{2\pi} dt \; u_E \; \hat{n} \cdot \nabla u_E \; , \tag{17b}$$

where

$$\nabla^2 u_I = 0 \; , \tag{18a}$$

$$\nabla^2 u_E = 0 \; , \tag{18b}$$

and, in addition to regularity, u_I and u_E satisfy boundary conditions at the plasma surface.

These boundary conditions are determined by the requirement that the perturbed magnetic field be tangent to the perturbed plasma surface, i.e.

$$(\hat{n} + \delta\hat{n}) \cdot [\underset{\sim}{B}(\underset{\sim}{r}_s + \delta\underset{\sim}{r}_s) + \underset{\sim}{b}(\underset{\sim}{r}_s + \delta\underset{\sim}{r}_s)] = 0 \ , \tag{19}$$

where $\delta\underset{\sim}{r}_s$ is the surface perturbation and $\delta\hat{n}$ the corresponding perturbation of the surface normal. Using $\delta\underset{\sim}{r}_s = \xi\ \hat{n}$ and expanding Eq. (19) to first order in ξ gives

$$\hat{n}\cdot\underset{\sim}{b}(\underset{\sim}{r}_s) + \delta\hat{n}\cdot\underset{\sim}{B}(\underset{\sim}{r}_s) + \xi\hat{n}(\hat{n}\cdot\nabla)\underset{\sim}{B}(\underset{\sim}{r}_s) = 0 \ . \tag{20}$$

Since ζ is an ignorable coordinate for the equilibrium, one can employ the ansatz $\xi = \xi(t)\ \exp(ik\ \zeta)$. Further, by the construction of the coordinates, the Jacobian of the transformation from η, t, ζ to cartesian $\underset{\sim}{r}$ is the constant area element A of Eq. (2), and $\hat{n}\cdot\nabla\hat{n} = \dfrac{\partial\hat{n}}{\partial\eta} = 0$. Thus, the last term of Eq. (20) may be written as

$$\xi\hat{n}\cdot(\hat{n}\cdot\nabla)\underset{\sim}{B} = \xi(\hat{n}\cdot\nabla)(\hat{n}\cdot\underset{\sim}{B}) = \xi\ \frac{\partial B^{\eta}}{\partial\eta} \ . \tag{21}$$

The right-hand side of Eq. (21) may be evaluated in terms of surface quantities by using $\nabla\cdot\underset{\sim}{B} = 0$:

$$\frac{\partial}{\partial t}\ AB^{t} + \frac{\partial}{\partial\eta}\ AB^{\eta} = 0 \ . \tag{22}$$

Combining Eqs. (21) and (22) yields

$$\xi \hat{n} \cdot (\hat{n} \cdot \nabla) \underset{\sim}{B} = - \xi \frac{\partial B^t}{\partial t} \quad . \tag{23}$$

The second term of Eq. (20) is evaluated by noting that the perturbed surface is given by $S = \eta - \xi = 0$. Thus,

$$\hat{n} + \delta\hat{n} = \frac{\nabla S}{|\nabla S|} = \hat{n} - \frac{\partial \xi}{\partial t} \nabla t - ik \xi \nabla z + O(\xi^2) \quad . \tag{24}$$

Combining Eqs. (20), (23), and (24) gives the boundary condition for the perturbed fields in the final simple form:

$$\hat{n} \cdot \underset{\sim}{b}_I = \frac{\partial u_I}{\partial \eta} = \frac{\partial}{\partial t}(B_I^t \xi) + ikB_I^\zeta \xi \quad , \tag{25a}$$

$$\hat{n} \cdot \underset{\sim}{b}_E = \frac{\partial u_E}{\partial \eta} = \frac{\partial}{\partial t}(B_E^t \xi) + ikB_E^\zeta \xi \quad . \tag{25b}$$

Given the displacement ξ, the perturbed potentials are found from the Neumann problems given by Eqs. (18) and (25). Then the plasma and vacuum energies are given by Eq. (17). By this means δW is expressed entirely in terms of ξ.

III. Low-β Analysis

The low-β analysis presented herein consists of two parts. First, the $O(\beta)$ corrections to the vacuum magnetic field are calculated. Next, the minimal δW is calculated through $O(\beta)$ by inserting the marginally stable vacuum perturbation into the surface contribution to δW. This calculation shows that the V'' criterion is precise in determining the sharp-boundary stability of low-β stellarators with no net current. However, systems without a magnetic well can be stabilized at low values of β by net current in the direction that increases the rotational transform difference between the exterior and the interior.

A. Equilibrium

The low-β equilibrium is obtained by expanding the various quantities α, γ, I, and Ψ of Sec. IIB as power series in β, e.g.

$$\alpha = 1 + \alpha_1 \beta \tag{26}$$

$$\gamma = \gamma_1 \beta \ , \tag{27}$$

and keeping the lowest order parts of each equation. From Eq. (11a), the internal equilibrium field is obtained,

$$B_{It} = (1+\alpha_1\beta) \frac{\partial \phi}{\partial t} = (1+\alpha_1\beta) B_{0t} \ . \tag{28a}$$

and

$$B_{I\zeta} = (1+\alpha_1\beta) = (1+\alpha_1\beta) B_{0\zeta} \ , \tag{28b}$$

in terms of the vacuum field components. Equation (11b) gives $B_{E\zeta}$ to

all orders in β. Expansion of Eq. (13) gives the remaining covariant components of the external magnetic field.

$$B_{Et} = B_{0t}(1+\alpha_1\beta) + \beta\left(\frac{1}{2B_0^t} + \frac{\alpha_1 B_0^\zeta}{B_0^t}\right) \tag{29}$$

At this point the axial current I or, equivalently γ, can be related to the parameter α. Ampere's law gives

$$\gamma_1 = \frac{1}{2\pi\beta}\int_0^{2\pi} dt\ B_{Et} = q_{h0}(V_0'/2 + \alpha_1/h)\ , \tag{30}$$

where q_{h0} and V_0' are calculated via Eqs. (C10) and (C15) using the vacuum fields. The coefficient γ_1 is arbitrary, but once it is specified the equilibrium is determined.

B. Stability

All perturbations of the vacuum field are stable or neutral ($\delta W \geqslant 0$). For infinitesimal β continuity demands that strictly stable perturbations ($\delta W > 0$) remain so. Hence, to determine stability only perturbations that are marginally stable in vacuum need to be examined to determine whether they become unstable with the introduction of pressure.

To find marginally stable vacuum perturbation, note from Eqs. (16) that the surface contribution to δW vanishes, while the plasma and vacuum contributions are non-negative definite. Thus, the only way for δW to vanish is for $\hat{n}\cdot\underset{\sim}{b}$ to vanish. This condition, together with Eqs. (25) yields the differential equation,

$$\frac{\partial}{\partial t}(B_0^t \xi_0) + ikB_0^\zeta \xi_0 = 0 \ , \tag{31}$$

for the marginally stable surface perturbation in vacuum. The solution to this equation is

$$\xi_0 = \exp(-ik\int^t dt\ B_0^\zeta/B_0^t)/B_0^t \ , \tag{32}$$

which is single valued only if

$$k = hK/q_{h0} \ , \tag{33}$$

where K is an integer. This perturbation is an interchange. It is constant on a field line, and its magnitude is proportional to the distance between field lines.

Since the vacuum is stable, the marginally stable perturbation ξ_0 is the minimizing perturbation. However, in the presence of a small plasma pressure, the minimizing perturbation is altered slightly, $\xi = \xi_0 + \beta\xi_1$. Upon inserting such a perturbation into Eq. (25a), one finds $\hat{n}\cdot\underset{\sim}{b}_I = O(\beta)$. This implies that $\delta W_P = O(\beta^2)$. Similarly, $\delta W_V = O(\beta^2)$. Therefore, through order β, only the surface term contributes to δW.

$$\delta W = \frac{A}{2}\int_0^{2\pi} dt\ |\xi|^2 \hat{n}\cdot\nabla\ \frac{1}{2}(|B_E|^2 - |B_I|^2) + O(\beta^2) \ . \tag{34}$$

This equation, in combination with Eqs. (B2) and (32), implies

$$\delta W_1 = \frac{A}{\beta} \int_0^{2\pi} dt \ (B_0^t)^{-2} \ B_0^j S_{jk} g^{k\ell} \Delta B_\ell \ , \tag{35}$$

where $\delta W = \beta \delta W_1 + O(\beta^2)$, and $\Delta B_\ell = B_{E\ell} - B_{I\ell}$. When the expressions for ΔB_ℓ calculated from Eqs. (11b), (28), and (29) are used, Eq. (35) reduces to

$$\delta W_1 = A \int_0^{2\pi} dt (B_0^t)^{-3} \ B_0^i S_{ij} [g^{jt}(1+\alpha_1 B_0^\zeta) - \alpha_1 g^{j\zeta} B_0^t] \ . \tag{36}$$

Finally, with the relation (30) between α_1 and γ_1 and the formulas (C13) and (C16) for shear and V'', Eq. (36) yields the simple result

$$\delta W_1 = 2\pi A^2 \ (\frac{q_h}{2} \frac{dV_0'}{dA_\zeta} + \frac{\gamma_1}{q_h} \frac{dq_h}{dA_\zeta}) \ . \tag{37}$$

The interpretation of Eq. (37) is straightforward. When no current is present ($\gamma_1 = 0$) the low-β stability of the system depends on dV'/dA_ζ. Since $q_h < 0$, the system is stable if dV'/dA_ζ is not positive. This is the familiar V'' criterion. Suppose instead that dV'/dA_ζ is positive. Then the system can be stabilized by a surface current $I_1 = \gamma_1/2\pi$ such that

$$\gamma_1 > - \frac{q_h^2}{2} \frac{dV'}{dA_\zeta} / \frac{dq_h}{dA_\zeta} = \frac{dV'}{dA_\zeta} / (\ell \frac{d\iota}{dA_\zeta}) \ . \tag{38}$$

Thus, if the shear is positive, γ_1 must be positive, i.e. the current must be in the direction that increases the rotational transform difference between the interior and the exterior.

IV. High-β Analysis

In this section, the equilibrium and stability analysis of the previous section is extended to arbitrary plasma β. First, a method for solving the Neumann potential problem in either the interior or the exterior of the plasma domain is developed. Next, this method is applied to determine the interior $\underset{\sim}{B}$ field. The exterior $\underset{\sim}{B}$ field is found without expansion in β as the solution of a quadratic. The requirement that this quadratic have a real solution determines an equilibrium β limit. Finally, the stability problem is formulated by expanding the surface displacement ξ and associated quantities as Fourier series in the poloidal coordinate t. Resulting matrix representations of δW are minimized by standard numerical techniques to give approximations to the normal mode frequencies (squared) of the system.

A. Solution of the Potential Problem

The formulation of the sharp boundary equilibrium and stability problems described in Section II leads to Neumann potential problems for the unperturbed and perturbed magnetic scalar potentials. These problems are transformed into integral equations and solved by a technique previously used.[5,6,12]

Consider the Neumann potential problem

$$\nabla^2\tilde{u} = 0 \quad ,$$

$$\hat{n}\cdot\nabla\tilde{u} = \tilde{f} \quad , \tag{39}$$

for either the interior or the exterior of the plasma domain. An

efficient and accurate algorithm for such problems is derived by combining Green's third identity with Fourier transform techniques.

When this identity is applied to the function pair consisting of the fundamental solution, $\tilde{G}$, of the Laplacian which is regular at ∞, and the unknown solution $\tilde{u}$, there results the integral equation[5,6]:

$$\tilde{u}(\underset{\sim}{r}) = \pm 2A \int dA(\underset{\sim}{r}') \left[\tilde{u}(\underset{\sim}{r}')\, \hat{n}'\cdot\nabla'\tilde{G}(\underset{\sim}{r},\underset{\sim}{r}') - \tilde{G}(\underset{\sim}{r},\underset{\sim}{r}')\, \hat{n}'\cdot\nabla'\tilde{u}(\underset{\sim}{r}')\right] , \quad (40)$$

where the integral is taken over the plasma surface, the normal is out of the plasma, and the upper (lower) sign holds for the interior (exterior) domain, respectively. The integral of Eq. (40) is to be interpreted in a principal value sense. The originally present δ-function singularity has been removed analytically.

With the coordinates of Sec. II, all equilibrium quantities are independent of the axial coordinate z. Because of this, it is convenient to Fourier analyze the surface quantities. Thus, $\tilde{u}(t,z,\eta=0) = \int dk\ \exp(ikz)\ u_k(t)$, $\tilde{f}(t,z,\eta=0) = \int dk\ \exp(ikz)\ f_k(t)$, and $\tilde{G}(t,z,\eta=0,t',z',\eta'=0) = \int dk\ \exp[ik(z-z')]\ G_k(t,t')$. Fixing k as a parameter for the subsequent discussion and suppressing k as a subscript, Eq. (40) may be Fourier decomposed to give

$$u(t) = \pm 2A \int_0^{2\pi} dt' \left[u(t')\, \hat{n}'\cdot\nabla'G(t,t') - G(t,t')\, f(t')\right] , \quad (41)$$

where G satisfies the fundamental equation

$$\nabla^2_{\underset{\sim}{k}}G(r,\varphi,r',\varphi') = \left(\frac{1}{r}\frac{\partial}{\partial r}\, r\, \frac{\partial}{\partial r} + \frac{1}{r^2}\frac{\partial^2}{\partial \varphi^2} - k^2 + 2ikh\frac{\partial}{\partial \varphi} + h^2\right) G$$

$$= \frac{1}{r'} \delta(r-r') \ \delta(\varphi-\varphi') \tag{42}$$

The solution of Eq. (42) regular at ∞ is easily expressed[12] in terms of the modified Bessel functions I, K as

$$G = -\frac{1}{2\pi} \sum_{p} I_{|p|}(|k-hp| \ r_<) \ K_{|p|}(|k-hp| \ r_>) \ e^{ip(\varphi-\varphi')} \quad , \tag{43}$$

where $r_< = \min(r,r')$ and $r_> = \max(r,r')$.

The one-dimensional integral equation, Eq. (41), is discretized by Fourier expansion of the unknown u as a function of t. This expansion converges rapidly and thus, when truncated and combined with fast Fourier transform techniques gives an accurate and efficient numerical scheme. Because of the ℓ-fold symmetry of the plasma surface in t, only harmonics which differ by an integer multiple of ℓ are coupled in the integral Eq. (41). Expanding

$$\begin{aligned} u(t) &= e^{iMt} \sum_{q} u_q e^{i\ell qt} \quad , \\ \hat{n}\cdot\nabla u(t) &= e^{iMt} \sum_{q} f_q e^{i\ell qt} \quad , \end{aligned} \tag{44}$$

gives the matrix problem

$$u_q = \pm \sum_{q'} N_{M+\ell q, M+\ell q'} u_{q'} \pm \sum_{q'} G_{M+\ell q, M+\ell q'} f_{q'} \quad , \tag{45}$$

where the matrix elements are

$$N_{nn'} = \frac{A}{\pi} \int_0^{2\pi} dt \int_0^{2\pi} dt' \ e^{-i(nt-n't')} \ \hat{n}'\cdot\nabla' G(t,t') \quad , \tag{46a}$$

$$G_{nn'} = -\frac{A}{\pi}\int_0^{2\pi} dt \int_0^{2\pi} dt'\; e^{-i(nt-n't')}\, G(t,t') \quad , \tag{46b}$$

A numerical solution of the potential problem of Eq. (39) is obtained by truncating the sums of Eq. (45) to a few harmonics (typically 20–40). Then N, G become finite matrices and the solution vector u is found by matrix inversion to be

$$u = \pm(1\mp N)^{-1} G\, f \quad . \tag{47}$$

Because of singularities in G, $\hat{n}'\cdot\nabla' G$ and slow convergence of the series of Eq. (43), the numerical evaluation of G, $\hat{n}'\cdot\nabla' G$ and the matrix elements of Eq. (46) requires some care. The details of these calculations are given in App. D.

B. Equilibrium

The determination of equilibrium surface quantities is described in this section. The method of Sec. IVA is used to solve Eq. (7) to determine Φ and hence the interior $\underset{\sim}{B}$ field on an arbitrary plasma surface. Then, the exterior $\underset{\sim}{B}$ field is found from equilibrium pressure balance. It is convenient to specify β and I and determine α from Eq. (14). The condition that Eq. (13) give a real B imposes an equilibrium β limit, β_c. For any particular plasma surface, β_c gives the value of plasma β below which equilibria exist.

From Eq. (47) with M = 0, the solution of Eq. (7) is obtained as:

$$\Phi = (1-N)^{-1} G\, f \quad , \tag{48}$$

where

$$f_q = -\frac{h}{2\pi A}\int_0^{2\pi} dt\; e^{-i\ell q t} r_s \dot{r}_s \quad ,$$

$$= -\frac{ih\,\ell q}{\pi A}\int_0^{2\pi} dt\; e^{-i\ell q t}\, r_s^2 \quad . \tag{49}$$

To simplify the calculation of the sequel, the plasma surface is assumed to have a reflection symmetry about t = 0. Thus, the parities

$$r_s(t) = r_s(-t) \quad ,$$

$$\varphi_s(t) = -\varphi_s(-t) \quad , \tag{50}$$

are assumed. Then f_q becomes an imaginary quantity and the Hermitian matrices N and G become real symmetric matrices. The real quantities $i\Phi_q$ are found by standard matrix techniques from Eq. (48). Then $\underset{\sim}{B}_0$ is evaluated by Fourier synthesis of $iq\,\Phi_q$ to obtain $\dot{\Phi}(t)$.

The equilibrium solution is completed by the specification of the two parameters β and I. Then α is determined by numerically finding the root of Eq. (14). This determines the covariant components of $\underset{\sim}{B}_I$ and $\underset{\sim}{B}_E$ from Eqs. (11) and (13).

The square root occuring in Eq. (13) constrains the allowable values of the equilibrium parameters β and I. Since the radicand must be positive, α^2 is constrained by

$$\alpha^2 > \alpha^2_{min} = \min_{0 \leq t \leq 2\pi} \frac{A^{-2} - \beta g^{tt}}{g^{tt} B_0^2} \quad . \tag{51}$$

Thus, since the right-hand side of Eq. (13) is a monotonically decreasing function of α^2,

$$I < I_{max} = -\int_0^{2\pi} \frac{dt}{g^{tt}} \left(g^{t\zeta} + \left(\beta g^{tt} + \alpha_{min}^2 g^{tt} B_0^2 - A^{-2} \right)^{1/2} \right) . \qquad (52)$$

The inequality of Eq. (52) determines the allowable values of the parameters β and I. If I = 0 is chosen, Eq. (52) is satisfied for $\beta = 0$ and for values of β less than some critical value, the equilibrium β limit, β_c. For values of β and I satisfying Eq. (52) equilibria exist and may be computed as described here.

C. Stability

To examine the stability of an arbitrary sharp boundary plasma, equilibrium surface quantities are determined as described in Sec. IVB. As a trial function, ξ is expanded in a Fourier series of several harmonics in t. The perturbed magnetic scalar potentials are similarly expanded and determined by the method of Sec. IVA. Combining all these expressions leads to a matrix representation of δW. The eigenvalues of this matrix are found by standard numerical techniques as approximations to the normal mode frequencies (squared) of the system.

Evaluation of δW as a functional of the surface displacement ξ is accomplished by expanding ξ as a Fourier series in t:

$$\xi = e^{iMt} \sum_m \xi_m e^{i\ell mt} . \qquad (53)$$

The surface term may be easily evaluated:

$$\delta W_S = \frac{1}{2} \sum_{m,m'} \xi_m^* \delta W_{Smm'} \xi_{m'} = \frac{A}{2} \xi^\dagger \delta \overleftrightarrow{W}_S \xi \quad , \tag{54}$$

where the * indicates complex conjugation, the † Hermitian conjugation, and ξ and δW_S are now written for the vector and matrix representations of these quantities. The matrix elements of Eq. (76) are given by

$$\delta W_{Smm'} = \frac{1}{2\pi} \int_0^{2\pi} dt \; e^{-i\ell(m-m')t}$$
$$\times \left[S_{tt} (B_E^t B_E^t - B_I^t B_I^t) + 2S_{t\zeta} (B_E^t B_E^\zeta - B_I^t B_I^\zeta) + S_{\zeta\zeta} (B_E^\zeta B_E^\zeta - B_I^\zeta B_I^\zeta) \right] \quad . \tag{55}$$

To obtain the corresponding matrix representation for δW_P and δW_V, the boundary conditions of Eq. (25) are Fourier analyzed. Thus, for δW_P, Eq. (25a) is analyzed as

$$\hat{n} \cdot \nabla u_I = e^{iMt} \sum_q f_{Iq} \; e^{i\ell qt}$$

so that

$$f_{Iq} = \frac{1}{2\pi} \int_0^{2\pi} dt \; e^{-i(M+\ell q)t} \left\{ \frac{\partial}{\partial t} (B_I^t \; \xi) + ikB_I^\zeta \; \xi \right\}$$
$$= i \sum_m F_{Iqm} \xi_m \quad , \tag{56}$$

or

$$f_I = i \; F_I \xi \quad , \tag{57}$$

where

$$F_{Iqm} = \frac{1}{2\pi} \int_0^{2\pi} dt\ e^{-i\ell(q-m)t} \{(M+\ell q)B_I^t + kB_I^\zeta\} \quad . \tag{58}$$

Note that F_{Iqm} is a real (non-square) matrix. The plasma energy is expressed using Eqs. (17), (47), and (57) as

$$\delta W_P = \frac{A}{2}\, u_I{}^\dagger f_I = \frac{A}{2}\, \xi^\dagger \delta \overleftrightarrow{W}_P \xi \quad , \tag{59}$$

where

$$\delta \overleftrightarrow{W}_P = F_I{}^\dagger (1-N)^{-1} G F_I \quad . \tag{60}$$

In a completely similar manner, the vacuum energy is given by

$$\delta W_V = \frac{A}{2}\, \xi^\dagger \delta \overleftrightarrow{W}_V\, \xi \quad , \tag{61}$$

where

$$\delta \overleftrightarrow{W}_V = F_E{}^\dagger (1+N)^{-1} G\, F_E \quad , \tag{62}$$

and

$$F_{Eqm} = \frac{1}{2\pi} \int_0^{2\pi} dt\ e^{-i\ell(q-m)t} \{(M+\ell q)B_E^t + kB_E^\zeta\} \quad . \tag{63}$$

To evaluate δW numerically, the Fourier transforms of Eqs. (55), (58), and (63) are carried out by fast Fourier transform techniques. Then Eqs. (60), and (62) are used to evaluate $\delta \overleftrightarrow{W}_P$, and

$\overleftrightarrow{\delta W}_V$. This gives the matrix representation of $\overleftrightarrow{\delta W} = \overleftrightarrow{\delta W}_S + \overleftrightarrow{\delta W}_P + \overleftrightarrow{\delta W}_V$. Because of truncation errors associated with truncating the sums over q, the numerical representations of $\overleftrightarrow{\delta W}_P$ and $\overleftrightarrow{\delta W}_V$ are not exactly symmetric. The order of accuracy is increased by replacing $\overleftrightarrow{\delta W}$ by the average of this numerical representation and its transpose. The resulting matrix representation of $\overleftrightarrow{\delta W}$ is real and symmetric.

The final step of minimizing with respect to the normal displacement is accomplished by finding the eigenvalues of the matrix $\overleftrightarrow{\delta W}$ by standard methods. The corresponding normalization (kinetic energy) is

$$T = \frac{A}{2}\, \xi^{\dagger}\xi \quad . \tag{64}$$

D. Applications

Using the equilibrium solution described in Sec. IVB above, a large number of $\ell = 1$, 2, and 3 configurations have been investigated for low-β stability. For vanishing axial current, I, low-β stability is equivalent to the existence of a magnetic well. The only configurations found which have such a well are $\ell = 1$ systems of the heliac type. The stabilization of a system with a magnetic hill by $I \neq 0$ has also been investigated.

Figure 2 shows the cross section of a stable $\ell = 1$ heliac configuration. For this case, h = 0.8 and the surface is given by

$$x_s(\tau) = \bar{x} + (r_0 + r_1 \cos\tau)\, \cos\gamma \tag{65}$$

$$y_s(\tau) = (r_0 + r_1 \cos\tau)\, \sin\gamma \tag{66}$$

$$\varphi_s(\tau) = \text{Arctan } y_s/x_s \tag{67}$$

$$\gamma = \varphi_1 \sin\tau \tag{68}$$

with $\bar{x} = 0.2$, $r_0 = 0.5$, $r_1 = 0.25$, $\varphi_1 = 1.6$. This is the same section chosen for the conducting boundary in an earlier, diffuse-profile, local mode stability study.[2]

The existence of a deep magnetic well for this configuration is confirmed by evaluation of δW_1 from Eq. (37). Evaluation of δW at finite β shows that the $\beta = 0$, marginal eigenmode indeed has ω^2 increasing linearly with β, and confirms that stability is acheived for all values of the axial wavenumber, k.

This low-β behavior persists as β is increased to quite large values. For the configuration shown in Fig. 2, stability for all k is realized up the the equilibrium β_c of 15%. These results are summarized in Fig. 3, where ω^2 vs. k is plotted for $\beta = 0$, 7.5%, and 15%.

To examine the stabilizing effect of $I \neq 0$ on a system with a magnetic hill, a previously studied[6] unstable $\ell = 3$ system is considered. Fig. 4 shows the cross section corresponding to $\delta = 0.24$ for the surface specified in Ref. 6. A helical wave number h = 0.3 was chosen and the plasma radius was taken as unity.

Evaluation of δW_1 confirms the low-β instability of this system with I = 0 and indicates that low-β stability requires $I = \beta I_1$, with $I_1 = 2.281$. Fig. 5 shows ω^2 vs. k for a small $\beta = 0.5\%$. The predicted current for stability is confirmed by the solid curve there. As the plasma β is increased, complete stability is realized for I nearly as predicted by δW_1. Figure 6 shows ω^2 vs. k for $\beta = 10\%$, a value close

to the equilibrium limit. The broken curve indicates complete stability for $I = 1.1\beta I_1$.

V. Conclusions

The free-boundary stability of straight, sharp-boundary stellarators is closely related to the vacuum field properties. If no net axial current is allowed to flow on the surface, stability is equivalent to the existence of a magnetic well. This seems realizable only for $\ell = 1$ heliac configurations. This low-β prediction is found to hold up to the equilibrium β limit, which is greater than 15% for a heliac with deep magnetic well.

The low-β analysis also predicts that any nontrivial configuration may be stabilized by adding a small net axial current. For a conventional $\ell = 3$ system this is shown to lead to a stable configuration with an average β of 10%.

These results for free-boundary stability, when taken together with earlier internal mode stability results, are extremely optimistic for the heliac configuration. The predicted stabilizing effect of axial current on conventional (non-heliac) stellarators should be investigated in a more realistic, diffuse equilibrium. The rather significant β values predicted by the simple model considered here might be realized in a hybrid toroidal system with small toroidal current.

Acknowledgments

This work was supported by the U.S. Department of Energy under grant No. DE-FG05--80ET-53088.

Appendix A

Geometry and Coordinates

The development of Sec. II relies on the coordinate system (η, t, ζ) as defined by Eqs. (1–3). In this appendix it is shown how the parameter t is found, and how the components of the metric tensor can be written in terms of the surface functions $r_s(t)$ and $\varphi_s(t)$.

For an arbitrary parameterization $r_s(\tau)$ an $\varphi_s(\tau)$ with $0 \leqslant \tau < 2\pi$, the surface area element is

$$\left|\frac{\partial \underset{\sim}{r}_s}{\partial \tau} \times \frac{\partial \underset{\sim}{r}_s}{\partial \zeta}\right| = \left[\left(\frac{\partial r_s}{\partial \tau}\right)^2\left(1 + h^2 r_s^2\right) + r_s^2 \left(\frac{\partial \varphi_s}{\partial \tau}\right)^2\right]^{1/2} .$$

It follows form this equation and Eq. (2) that t and τ satisfy the relation,

$$A \frac{dt}{d\tau} = \left[\left(\frac{\partial r_s}{\partial \tau}\right)^2\left(1 + h^2 r_s^2\right) + r_s^2 \left(\frac{\partial \varphi_s}{\partial \tau}\right)^2\right]^{1/2} . \tag{A1}$$

The requirement that t increase by 2π when τ increases by 2π determines A to be

$$A = \frac{1}{2\pi} \int_0^{2\pi} d\tau \left[\left(\frac{\partial r_s}{\partial \tau}\right)^2\left(1 + h^2 r_s^2\right) + r_s^2 \left(\frac{\partial \varphi_s}{\partial \tau}\right)^2\right]^{1/2} . \tag{A2}$$

After determining A from Eq. (A2), $t(\tau)$ can be found by integrating Eq. (A1).

The surface unit normal is given in the usual way via

$$\hat{n} = A^{-1} \frac{\partial r_s}{\partial t} \times \frac{\partial r_s}{\partial \zeta} \quad . \tag{A3}$$

From this is obtained the normal derivative operator,

$$\hat{n} \cdot \nabla = A^{-1} \left[r_s \dot{\varphi}_s \frac{\partial}{\partial r} - (\dot{r}_s / r_s)(1 + h^2 r_s^2) \frac{\partial}{\partial \varphi} + h r_s \dot{r}_s \frac{\partial}{\partial z} \right] . \tag{A4}$$

The elements of the covariant metric tensor are found from $g_{ij} = \partial_i r \cdot \partial_j r$. This formula, together with Eq. (3) gives the following values,

$$\begin{aligned} g_{\eta\eta} &= 1 \quad , & g_{\eta t} &= 0 \quad , \\ g_{tt} &= \dot{r}_s^2 + r_s^2 \dot{\varphi}_s^2 \quad , & g_{t\zeta} &= h r_s^2 \dot{\varphi}_s \quad , \\ g_{\zeta\zeta} &= 1 + h^2 r_s^2 \quad , & g_{\zeta\eta} &= 0 \quad , \end{aligned} \tag{A5}$$

for the metric tensor elements on the surface. As usual, the contravariant metric tensor is found by matrix inversion. The resulting expressions on the surface are

$$\begin{aligned} g^{\eta\eta} &= 1 \quad , & g^{\eta t} &= 0 \quad , \\ g^{tt} &= A^{-2}(1 + h^2 r_s^2) \quad , & g^{t\zeta} &= -A^{-2} h r_s^2 \dot{\varphi}_s \quad , \\ g^{\zeta\zeta} &= A^{-2}(\dot{r}_s^2 + r_s^2 \dot{\varphi}_s^2) \quad , & g^{\zeta\eta} &= 0 \quad . \end{aligned} \tag{A6}$$

From these results it follows that the volume element is simply A.

Appendix B

The Normal Gradient of the Dot Product of Two Tangent Curl-Free Vectors

A formula useful for calculating δW_S expresses the normal gradient of the dot product of any two tangent, curl-free fields in terms of their surface values. Let $\underset{\sim}{P}$ and $\underset{\sim}{Q}$ satisfy $\nabla\times\underset{\sim}{P} = \nabla\times\underset{\sim}{Q} = 0$ and $\hat{n}\cdot\underset{\sim}{P} = \hat{n}\cdot\underset{\sim}{Q} = 0$ on the surface. Then $\hat{n}\cdot\nabla\underset{\sim}{P}\cdot\underset{\sim}{Q} = \frac{\partial}{\partial\eta} P^j g_{jk} Q^k$ with the usual summation over repeated indices understand. Thus,

$$\hat{n}\cdot\nabla\underset{\sim}{P}\cdot\underset{\sim}{Q} = -P^j\left(\frac{\partial}{\partial\eta} g_{jk}\right)Q^k + \left(\frac{\partial}{\partial\eta} g_{jk}P^j\right)Q^k + P^j\left(\frac{\partial}{\partial\eta} g_{jk}Q^k\right) \quad . \tag{B1}$$

The vanishing of the last two terms of Eq. (B1) follows from $\nabla\times\underset{\sim}{P} = 0$. That is,

$$\frac{\partial}{\partial\eta} g_{jk}P^j = \partial_k g_{\eta j}P^j = 0 \quad ,$$

since $g_{\eta j} = 0$ unless $j = \eta$, but $P^\eta = \hat{n}\cdot\underset{\sim}{P} = 0$ by assumption. Thus,

$$\frac{1}{2}\,\hat{n}\cdot\nabla\underset{\sim}{P}\cdot\underset{\sim}{Q} = P^j S_{jk} Q^k \quad , \tag{B2}$$

where

$$S_{jk} = -\frac{1}{2}\frac{\partial}{\partial\eta} g_{jk} \quad , \tag{B3}$$

and the indices j,k assume only the values t,ζ.

This matrix is calculated by using the identities, $g_{jk} = \partial_j \underset{\sim}{r} \cdot \partial_k \underset{\sim}{r}$ and $\hat{n} = \frac{\partial \underset{\sim}{r}}{\partial \eta}$:

$$S_{jk} = -\frac{1}{2}\left(\partial_j \hat{n} \cdot \partial_k \underset{\sim}{r} + \partial_j \underset{\sim}{r} \cdot \partial_k \hat{n}\right) .$$

The required derivatives of $\hat{n}$ may be computed from Eq. (4) to give the final form of S_{jk}:

$$S_{tt} = A^{-1}\left(r_s \dot{\varphi}_s \dot{r}_s^{\bullet} - 2\dot{r}_s^2 \dot{\varphi}_s - r_s^2 \dot{\varphi}_s^3 - r_s \dot{r}_s \dot{\varphi}_s^{\bullet}\right) ,$$

$$S_{tz} = -A^{-1} h(r_s^{\bullet 2} + r_s^2 \dot{\varphi}_s^2) ,$$

$$S_{zz} = -A^{-1} h^2 r_s^2 \dot{\varphi}_s . \qquad \text{(B4)}$$

Appendix C

Vacuum Field Properties

In this appendix several properties of helically symmetric vacuum fields are discussed. It is shown that the contravariant component B^t, the component in the surface but not in the symmetry direction, is negative. Next, the calculation of the magnetic well and the shear are discussed. Finally, it is shown that q_h is negative, which implies that vacuum rotational transform per field period, ι, is always less than $1/\ell$.

1. Sign of B^t

A flux function must have the property that any magnetic field line is confined to one of its contours. It follows from the ignorability of the original coordinate z of (r,φ,z) and the method of construction, that the new coordinate ζ of (η,t,ζ) is ignorable. This implies that the vector potential can be chosen such that its covariant components do not depend on ζ.

$$\underset{\sim}{A} = A_\eta(\eta,t)\nabla\eta + A_t(\eta,t)\nabla t + A_\zeta(\eta,t)\nabla\zeta \qquad (C1)$$

For such a vector potential $\underline{B} \cdot \nabla A_\zeta = 0$. Hence, A_ζ (the helical flux) is a flux function.

Computing the magnetic field from Eq. (C1) and using the usual formulae of differential geometry yields

$$B^t = -\frac{\partial A_\zeta}{\partial \eta}/A \ , \qquad (C2)$$

where the unsubscripted A is simply the area of Sec. II. Equation (C2) tells us that the flux surface spacing is proportional to $(B^t)^{-1}$. This also shows that B^t must not change sign. Were it to change sign, Eq. (C2) would imply that a surface of a slightly different value of A_ζ would be inside the present surface for some values of t and outside for other values.

The sign of B^t is determined by considering the equation,

$$B^t = A^{-2}\left[(1+h^2r_s^2)\,\frac{\partial\phi}{\partial t} - hr_s^2\,\dot{\varphi}_s\right] , \tag{C3}$$

which comes from using the metric tensor (A5) to calculate B^t from the covariant components of B as given by Eq. (6). Dividing this equation by the factor $A^{-2}(1+h^2r_s^2)$ and integrating over t, one obtains

$$A^2 \int_0^{2\pi} dt\; B^t/(1+h^2r_s^2) = -\int_0^{2\pi} dt\; hr_s^2\dot{\varphi}_s/(1+h^2r_s^2) . \tag{C4}$$

The integral on the right side of Eq. (C4) is simply the area integral of $2h/(1+h^2r_s^2)$ over a constant-z cross-section of the stellarator:

$$\int_0^{2\pi} dt\; hr_s^2\dot{\varphi}_s/(1+h^2r_s^2) \;=\; \int d\varphi dr\; 2hr/(1+h^2r^2) .$$

As this integral is manifestly positive, Eq. (C4) indicates that a certain average of B^t is negative. Since B^t cannot change sign, it must be negative for all values of t. This fact, together with Eq. (C2) shows that A_ζ increases outward.

2. Rotational transform

The rotational transform per field period is defined by the formula,

$$\iota = \lim_{\Delta\zeta\to\infty} \left(\ell^{-1} + \frac{\Delta t}{h\ell\Delta\zeta} \right) , \tag{C5}$$

where Δt and $\Delta\zeta$ are the changes in the coordinates t and ζ as one moves along a field line. This formula is easily remembered if one notes that a point at a fixed value of t has a rotational transform per field period of $1/\ell$. The periodicity in t and lack of dependence on ζ allows the inverse helical transform to be calculated explicitly,

$$q_h \equiv \lim_{\Delta\zeta\to\infty} \frac{h\Delta\zeta}{\Delta t} = \frac{h}{2\pi} \int_0^{2\pi} dt \; B^\zeta / B^t . \tag{C6}$$

Combining Eqs. (C5) and (C6) yields

$$\iota = \left(1+q_h^{-1}\right)/\ell . \tag{C7}$$

3. Sign of q_h

To prove that q_h is negative for a vacuum field, we use the integral form of Ampere's law;

$$\oint \underline{B} \cdot \underline{d\ell} = 0 . \tag{C8}$$

The path of integration consists of two pieces. The first piece starts

at (t=0, ζ=0) and moves along a field line to $t = 2\pi$ at which point $h\zeta = 2\pi q_h$, according to Eq. (C6). The second part of the path stays at a constant value of $t = 2\pi$. It starts at the endpoint of the first path $\xi = 2\pi q_h$, and it ends at the beginning of the first path. For this path, Eq. (C8) becomes

$$\int_0^{2\pi} dt\ \underline{B} \cdot \frac{d\underline{\ell}_f}{dt} + \int_{2\pi q_h/h}^{0} d\zeta\ B_\zeta = 0 \ , \tag{C9}$$

where $d\underline{\ell}_f/dt = \partial\underline{\ell}/\partial t + (B^\zeta/B^t)\partial\underline{\ell}/\partial\zeta$ describes the field line path through real space. With our normalization, $B_\zeta = 1$, and Eq. (C9) reduces to

$$q_h = \frac{h}{2\pi}\int_0^{2\pi} dt\, |B|^2/B^t \ , \tag{C10}$$

which, since $B^t<0$, shows that q_h is negative.

4. Shear

The shear parameter is defined to be the derivative of the rotational transform with respect to the helical flux.

$$\frac{d\iota}{dA_\zeta} = -\frac{1}{\ell q_h^2}\frac{dq_h}{dA_\zeta} \tag{C11}$$

From Eq. (C6)

$$\frac{dq_h}{dA_\zeta} = \frac{h}{2\pi}\int_0^{2\pi} dt\ \left(B^t\ \frac{\partial B^\zeta}{\partial A_\zeta} - B^\zeta\ \frac{\partial B^t}{\partial A_\zeta}\right)/(B^t)^2\ ,$$

which yields

$$\frac{dq_h}{dA_\zeta} = -\frac{h}{2\pi A}\int_0^{2\pi}\frac{dt}{(B^t)^3}\left(B^t\ \frac{\partial B^\zeta}{\partial \eta} - B^\zeta\ \frac{\partial B^t}{\partial \eta}\right)\ . \tag{C12}$$

This expression can be further reduced by using the identity (B2). For example,

$$\frac{\partial B^\zeta}{\partial \eta} = \frac{\partial}{\partial \eta}\ (\underline{B}\cdot\nabla\zeta) \ = \ 2B^j S_{jk}(\nabla\zeta)^k = 2B^i S_{jk} g^{k\zeta}\ .$$

Application of this result and the companion expression for $\partial B^t/\partial\eta$ to Eq. (C12) yields

$$\frac{dq_h}{dA_\zeta} = -\frac{h}{2\pi A}\int_0^{2\pi}\frac{dt}{(B^t)^3}\left\{B^t B^i S_{ij} g^{j\zeta} - B^\zeta B^i S_{ij} g^{jt}\right\}\ . \tag{C13}$$

5. Specific volume, V'

The specific volume V', which is the derivative of the volume enclosed by a flux surface with respect to the toroidal flux, can be put in the form,

$$V' = \lim_{s\to\infty}\frac{\int_0^s ds/B}{h[z(s)-z(0)]}\ , \tag{C14}$$

where s parameterizes distance along a field line, and z(s) gives the value of the z-coordinate of a point moving along that field line. With periodicity the following expression for V' is obtained.

$$V' = q_h^{-1} \int_0^{2\pi} \frac{dt}{2\pi} (B^t)^{-1} \tag{C15}$$

6. Stability factor, V''

The stability factor V'' is the derivative of V' with respect to toroidal flux. Here it is more convenient to use the derivative of V' with respect to helical flux. The previously introduced techniques yield

$$\frac{dV'}{dA_\zeta} = - q_h^{-1} \frac{dq_h}{dA_\zeta} V' + q_h^{-1} \int_0^{2\pi} \frac{dt}{2\pi A} B^i S_{ij} g^{jt} / (B^t)^3 \ . \tag{C16}$$

Since toroidal flux and helical flux both increase outward, dV'/dA_ζ and V'' have the same sign.

Appendix D

Evaluation of the Green's Matrices

In this appendix, the numerical procedure used to evaluate the matrix elements of Eq. (46) is outlined. The evaluation of these elements involves four major tasks. First the modified Bessel functions and their derivatives must be evaluated for the calculation of the sum of Eq. (43) and the corresponding series representation of $\hat{n}' \cdot \nabla' G(t,t')$. Second, the convergence of these series is unacceptably slow and must be accelerated by subtracting the asymptotic term from the general term and summing the asymptotic series analytically. Third, the integrands of Eq. (46) contain logarithmic singularities at $t=t'$; these are resolved by adding and subtracting a quantity with the same singularity whose Fourier integral is known. Finally, the ℓ-fold periodicity of equilibrium quantities causes a decoupling of harmonics which differ by other than an integral multiple of ℓ; the efficiency of the calculation is increased by accounting for this symmetry.

1. Modified Bessel Functions

It is convenient to scale the modified Bessel functions so that the numerically computed scaled quantities are of order unity. Thus, instead of I_p, K_p and their derivatives, the scaled quantities

$$\hat{I}_p(z) = \frac{p!}{(z/2)^p} I_p(z) \ , \tag{D1a}$$

$$\hat{I}'_p(z) = \frac{p!}{(z/2)^p} I'_p(z) \ , \tag{D1b}$$

$$\hat{K}_p(z) = \frac{(z/2)^p}{p!} K_p(z) \ , \tag{D1c}$$

$$\hat{K}'_p(z) = \frac{(z/2)^p}{p!} K'_p(z) \ , \tag{D1d}$$

are computed. Note that $\hat{I}'_p, \hat{K}'_p$ are not the derivatives of $\hat{I}_p, \hat{K}_p$. These scaled quantities are bounded as $z \to 0$ and grow only geometrically as $p \to \infty$ with $z = p\zeta$, ζ of order unity.

The scaled modified Bessel functions of Eq. (D1) are evaluated from the following recurrence relations[14]

$$\hat{I}_{p+1}(z) = \frac{4p(p+1)}{z^2} [\hat{I}_{p-1}(z) - \hat{I}_p(z)] \ , \tag{D2a}$$

$$\hat{K}_{p+1}(z) = \frac{p}{p+1} \hat{K}_p(z) + \frac{z^2}{4p(p+1)} \hat{K}_{p-1}(z) \ , \tag{D2b}$$

$$\hat{I}'_p(z) = \frac{z}{2(p+1)} \hat{I}_{p+1}(z) + \frac{p}{z} \hat{I}_p(z) \ , \tag{D2c}$$

$$\hat{K}'_p(z) = -\frac{2(p+1)}{z} \hat{K}_{p+1}(z) + \frac{p}{z} \hat{K}(z) \ . \tag{D2d}$$

Once $\hat{K}_0$ and $\hat{K}_1$ are evaluated by polynomial approximation[14], Eq. (D2b) is iterated forward with $p = 1,2,\ldots$ until the desired order is reached. A similar iteration of Eq. (D2a) is unstable. Thus, Eq. (D2a) is iterated backward from $p = \infty$ using a continued fraction technique[15].

2. Acceleration of Series Convergence

The series of Eq. (43) expresses the desired Green's function in terms of the scaled modified Bessel functions. For r close to r', however, the terms of the series decay only as $1/|p|$ so that an excessively large number of terms is required to obtain G to sufficient accuracy.

To obtain an efficient summation technique, the asymptotic form of the general term in Eq. (43) is subtracted from the general term and the resulting difference series summed numerically. The series of the asymptotic term is summed analytically is terms of elementary functions and added to the difference series to obtain G.

Thus

$$G = g+H \tag{D3}$$

where

$$g = \sum_{p} g_p \, e^{ip(\varphi-\varphi')} \ , \tag{D4a}$$

$$g_0 = -\frac{1}{2\pi}\left(\hat{I}_0\hat{K}_0 - \frac{1}{2}\sqrt{T_<T_>}\,\log u\right) , \tag{D4b}$$

$$g_p = -\frac{1}{2\pi}\left[\hat{I}_{|p|}\hat{K}_{|p|} - \frac{1}{2}\sqrt{T_<T_>}\,\frac{\lambda^{\sigma}\,u^{|p|}}{|p|}\right] \ , \ p\neq 0 \tag{D4c}$$

In Eq. (D4), the arguments of $\hat{I},\hat{K}$ are as in Eq. (43), σ = sign p, and,

$$T_< = 1/(1+h^2r_<^2)^{1/2} \tag{D5a}$$

$$T_> = 1/(1+h^2r_>^2)^{1/2} \ , \tag{D5b}$$

$$u = \frac{r_<}{r_>} \frac{1+(1+h^2r_>^2)^{1/2}}{1+(1+h^2r_<^2)^{1/2}} \exp\left[(1+h^2r_<^2)^{1/2} - (1+h^2r_>^2)^{1/2}\right] , \tag{D5c}$$

$$\lambda = \exp \frac{k}{h}\left[(1+h^2r_>^2)^{1/2} - (1+h^2r_<^2)^{1/2}\right] . \tag{D5d}$$

The remaining term in Eq. (D3) is the sum of the asymptotic terms:

$$H = -\frac{1}{4\pi}\sqrt{T_<T_>}\left[\log u + \sum_{p\neq 0} \frac{\lambda^\sigma u^{|p|}}{|p|} e^{ip(\varphi-\varphi')}\right]$$

$$= -\frac{1}{4\pi}\sqrt{T_<T_>}\left[\log u - \lambda \log(1-z) - \lambda^{-1}\log(1-z^*)\right] , \tag{D6}$$

where

$$z = ue^{i(\varphi-\varphi')} \tag{D7}$$

and the * indicates complex conjugation.

For p large, the asymptotic expression[14] for $\hat{I}_p, \hat{K}_p$ show that $g_p \sim 1/p^2$. Thus, the series of Eq. (D4a) converges sufficiently rapidly that an accurate numerical sum may be evaluated using 10 to 50 terms (the required number depends on ℓ and the surface shape).

A similar acceleration scheme is applied to the series representations for $\partial G/\partial r'$, $\partial G/\partial \varphi'$. Thus

$$\frac{\partial G}{\partial r'} = g_{r'} + H_{r'} , \tag{D8a}$$

$$\frac{\partial G}{\partial \varphi'} = g_{\varphi'} + H_{\varphi'} , \tag{D8b}$$

where

$$g_{r'} = \sum g_{r'p}\, e^{ip(\varphi-\varphi')} \quad , \tag{D9a}$$

$$g_{\varphi'} = \sum g_{\varphi'p}\, e^{ip(\varphi-\varphi')} \quad , \tag{D9b}$$

$$g_{r'0} = -\frac{1}{2\pi}\left[w_0 - \frac{1}{2}\sqrt{T_{<}T_{>}}\,(D_u + D_T \log u)\right] \quad , \tag{D10a}$$

$$g_{r'p} = -\frac{1}{2\pi}\left[w_p - \frac{1}{2}\sqrt{T_{<}T_{>}}\,\lambda^{\sigma}\, u^{|p|}\left(D_u + \frac{D_T + \sigma D_\lambda + a_\sigma D_u}{|p|}\right)\right] \quad , \; p\neq 0 \tag{D10b}$$

$$g_{\varphi'0} = 0 \quad , \tag{D10c}$$

$$g_{\varphi'p} = \frac{i}{2\pi}\left[p\hat{I}_p\hat{K}_p - \frac{1}{2}\sqrt{T_{<}T_{>}}\,\lambda^{\sigma}\, u^{|p|}\left(\sigma + \frac{a_\sigma}{p}\right)\right] \quad , \; p\neq 0 \quad . \tag{D10d}$$

In Eq. (D10)

$$w_p = |k-hp| \qquad \begin{matrix} \hat{I}_p'\,\hat{K}_p \;, & r' < r \\ \hat{I}_p\,\hat{K}_p' \;, & r' > r \end{matrix} \quad , \tag{D11a}$$

$$D_u \equiv \frac{1}{u}\frac{\partial u}{\partial r'} \quad , \tag{D11b}$$

$$D_\lambda \equiv \frac{1}{\lambda}\frac{\partial \lambda}{\partial r'} \quad , \tag{D11c}$$

$$D_T \equiv \left[T_{<}T_{>}\right]^{-1/2} \cdot \frac{\partial}{\partial r'}\left[T_{<}T_{>}\right]^{1/2} \quad , \tag{D11d}$$

and

$$a_{\pm} \equiv \frac{3T_<-5T_<^3}{24} - \frac{k^2T_<}{2h^2} - \frac{3T_>-5T_>^3}{24} + \frac{k^2T_>}{2h^2} \pm \frac{kh}{2}\left(r_>^2T_>^2 + r_<^2T_<^2\right) . \qquad \text{(D11e)}$$

The remaining term in Eq. (D8) are the sums of the asymptotic terms:

$$H_r' = -\frac{1}{4\pi}\sqrt{T_<T_>}\left\{D_u\left[1 + \frac{\lambda z}{1-z} + \frac{z^*}{\lambda(1-z^*)}\right] + D_T \log u\right.$$

$$\left. - (D_T+D_\lambda+a_+D_u)\lambda\log(1-z) - (D_T-D_\lambda+a_-D_u)\lambda^{-1}\log(1-z^*)\right\} , \qquad \text{(D12a)}$$

$$H_\varphi' = \frac{i}{4\pi}\sqrt{T_<T_>}\left[\frac{\lambda z}{1-z} - \frac{z^*}{\lambda(1-z^*)} - \lambda a_+\log(1-z) + \lambda^{-1}a_-\log(1-z^*)\right] . \qquad \text{(D12b)}$$

Combining Eq. (D8) with Eq. (7) gives the required expression for the normal gradient of G:

$$A\,\hat{n}'\cdot\nabla' G = g_n' + H_n' , \qquad \text{(D13a)}$$

where

$$g_n' = r'\dot{\varphi}'\,g_r' - \frac{\dot{r}'}{r'}(1+h^2r'^2)g_\varphi' - ikhr'\dot{r}'g , \qquad \text{(D13b)}$$

$$H_n' = r'\dot{\varphi}'\,H_r' - \frac{\dot{r}'}{r'}(1+h^2r'^2)H_\varphi' - ikhr'\dot{r}'H . \qquad \text{(D13c)}$$

The acceleration scheme described here is a simplification of that described in Ref. 12 in that only terms of order $|p|^{-1}$ are added and subtracted from the general terms. Because of this, the accuracy obtained when a given number of terms are summed numerically is

reduced. It has been found that this may be easily compensated by increasing the number of terms included by a modest amount.

3. Resolution of the Logarithmic Singularities

The construction of the series of Eqs. (D4) and (D9) assures that $g, g_n,$ are continuous at $t=t'(r=r', \varphi=\varphi')$. The remainder series $H, H_n,$, however, have logarithmic singularities (in addition to the δ function singularity already explicitly removed in Sec. IV). After extensive algebra it is found that

$$H - \frac{T'}{2\pi} \log\left|\sin \frac{1}{2}(t-t')\right| \sim \frac{T'}{2\pi} \log \frac{2A}{r'} , \tag{D14a}$$

$$H_n' + \frac{h^2 r'^2 \dot{\varphi}'}{4\pi(1+h^2 r'^2)^{3/2}} \log\left|\sin \frac{1}{2}(t-t')\right|$$

$$\sim \frac{1}{4\pi(1+h^2 r'^2)^{1/2}} \left\{A^{-2}\left[\dot{r}' r'^2 \dot{\varphi}' + r'(1+h^2 r'^2)(\dot{r}'\ddot{\varphi}' - \ddot{r}'\dot{\varphi}')\right]\right.$$

$$\left. - 2ikhr'\dot{r}' - \frac{h^2 r'^2 \dot{\varphi}'}{1+h^2 r'^2} \log \frac{2A}{r'}\right) , \tag{D14b}$$

where

$$T' = 1/(1+h^2 r'^2)^{1/2} , \tag{D14c}$$

in the sense that the difference between the right- and left-hand members of the approximate equalities tend to zero continuously as $t \to t'$.

To numerically evaluate the Fourier integrals of Eq. (65), fast Fourier transform technique are applied to the continuous functions

$$\hat{G} = g+H - \frac{T'}{2\pi} \log\left|\sin \frac{1}{2} (t-t')\right| , \tag{D15a}$$

$$\hat{N} = g_{n'}+H_{n'} + \frac{h^2 r'^2 \dot{\varphi}'}{4\pi(1+h^2 r'^2)^{3/2}} \log\left|\sin \frac{1}{2} (t-t')\right| . \tag{D15b}$$

These functions are evaluated for $t \neq t'$ by the expressions of Eqs. (D4), (D6), (D9), (D12), and (D13). For $t = t'$, the right-hand sides of Eqs. (D14) replaces the indeterminant differences of H, H_n, and the logarithmic terms in Eqs. (D15).

The desired matrix elements are evaluated by adding the transforms of the logarithmic terms in Eqs. (D15). Thus

$$N_{nn'} = \frac{1}{\pi} \int_0^{2\pi} dt \int_0^{2\pi} dt' \, e^{i(nt-n't')} \hat{N}$$

$$+ \frac{h^2}{8\pi} \delta_n \int_0^{2\pi} dt' \, e^{-i(n-n')t'} \frac{r'^2 \dot{\varphi}'}{(1+h^2 r'^2)^{3/2}} , \tag{D16a}$$

$$G_{nn'} = \frac{A}{\pi} \int_0^{2\pi} dt \int_0^{2\pi} dt' \, e^{-i(nt-n't')} \hat{G}$$

$$- \frac{A}{4\pi} \delta_n \int_0^{2\pi} dt' \, e^{-i(n-n')t'} T' , \tag{D16b}$$

where

$$\delta_0 = \log 2 , \tag{D17a}$$

$$\delta_n = \frac{1}{2|n|} , \quad n \neq 0 . \tag{D17b}$$

4. ℓ-fold Symmetry

The Fourier transforms of Eqs. (D16) are of the form

$$K_{qq'} = \frac{1}{\pi}\int_0^{2\pi} dt \int_0^{2\pi} dt' \; e^{-iM(t-t')}\; e^{-i\ell(qt-q't')} K(t,t') \qquad \text{(D18a)}$$

where

$$K = Q + \sum_p R_p(r,r')\; e^{ip(\varphi-\varphi')} \; . \qquad \text{(D18b)}$$

The equilibrium periodicity properties

$$r(t+2\pi/\ell) = r(t) \; , \qquad \text{(D19a)}$$

$$\varphi(t+2\pi/\ell) = \varphi(t) + 2\pi/\ell \; , \qquad \text{(D19b)}$$

may be used to reduce the integral of Eq. (D18a) to the following:

$$K_{qq'} = \frac{1}{\pi}\int_0^{2\pi} d\tau \int_0^{2\pi} d\tau' \; e^{-i(q\tau-q'\tau')}\; L(\tau,\tau') \; , \qquad \text{(D20a)}$$

where L is a compressed doubly periodic functions of τ,τ' with periods 2π, 2π given by:

$$L(\tau,\tau') = \exp\left[-\frac{iM}{\ell}(\tau-\tau')\right]\left(\frac{1}{\ell}\sum_{m=0}^{\ell-1} \exp\left(i\,\frac{2\pi mM}{\ell}\right) Q\left(\frac{\tau}{\ell},\; \frac{\tau'+2\pi m}{\ell}\right)\right.$$

$$\left.\sum_p R_{M+\ell p}\; \exp\left\{i(M+\ell p)\left[\varphi\left(\frac{\tau}{\ell}\right) - \varphi\left(\frac{\tau'}{\ell}\right)\right]\right\}\right) \; . \qquad \text{(D20b)}$$

Note that the equilibrium periodicity properties insure that L is a doubly periodic function.

For the same accuracy, the evaluation of $K_{qq'}$ using L requires only $1/\ell^3$ the number of R evaluations as that using K. The procedure of Eqs. (D20) is thus applied to the transforms of Eqs. (D16) with a large reduction of computations for $\ell > 1$.

Figure Captions

Figure 1: Coordinates for sharp boundary calculation. r,φ,z are helical coordinates. η,t,ζ are surface coordinates.

Figure 2: Cross-section of a stable heliac configuration.

Figure 3: Eigenvalue ω^2 as a function of axial wavenumber k for $\beta = 0.0$ (solid curve), 0.075 (dashed curve), and 0.15 (dotted curve) for the heliac configuration.

Figure 4: Cross-section of an unstable $\ell = 3$ configuration.

Figure 5: Eigenvalue ω^2 as a function of axial wavenumber k at $\beta = 0.005$ and I=0 (dotted curve), $I = \beta I$, (solid curve), and $I = 2\beta I$, (dashed curve) for the $\ell = 3$ configuration.

Figure 6: Eigenvalue ω^2 as a function of axial wavenumber k at $\beta = 0.10$ and I = 0 (dotted curve), $I = \beta I_1$, (solid curve), and $I = 1.1\beta I_1$ (dashed curve) for the $\ell = 3$ configuration.

References

1. S. Yoshikawa, Bull. Am. Phys. Soc. 26, 891(1981).
2. D. A. Monticello and R. L. Dewar, Annual Controlled Fusion Theory Conference (Santa Fe, New Mexico, 1982) paper 3C8.
3. R. C. Davidson and J. P. Freidberg, in Proceedings of the Third Topical Conference on Pulsed High Beta Plasmas (Culham Laboratory, Culham, England, 1975) paper A1.5 .
4. H. Grad and H. Weitzner, Phys. Fluids 12, 1725(1969).
5. J. P. Freidberg, Phys. Fluids 16, 1349(1973).
6. J. P. Freidberg, W. Grossman, and F. A. Haas, Phys. Fluids 19, 1599(1976).
7. I. B. Bernstein, E. A. Frieman, M. D. Kruskal, and R. M. Kulsrud, Proc. Roy. Soc. A244, 2(1958).
8. M. N. Rosenbluth and C. L. Longmire, Ann. Phys. (N.Y.) 1, 120(1957).
9. J. L. Johnson and J. M. Greene, Plasma Phys. 9, 611(1967).
10. H. P. Furth, J. Killeen, M. N. Rosenbluth, and B. Coppi, in Plasma Physics and Controlled Nuclear Fusion Research, Vol. I, IAEA (Vienna, 1966) p.103.
11. B. McNamara, K. J. Whiteman, and J. B. Taylor, in Plasma Physics and Controlled Nuclear Fusion Research, Vol. I, IAEA (Vienna, 1966) p.145.
12. P. Merkel, Z. Naturforsch. 37a, 859(1982).
13. R. Courant and D. Hilbert, Methods of Mathematical Physics, (Interscience, New York, 1962) Vol. II, p.252.

14. F. W. J. Olver, in Handbook of Mathematical Functions, M. Abramowitz and I. A. Stegun, eds. (Dover, New York, 1968).

15. G. Blanch, SIAM Rev. 6, 383(1964).

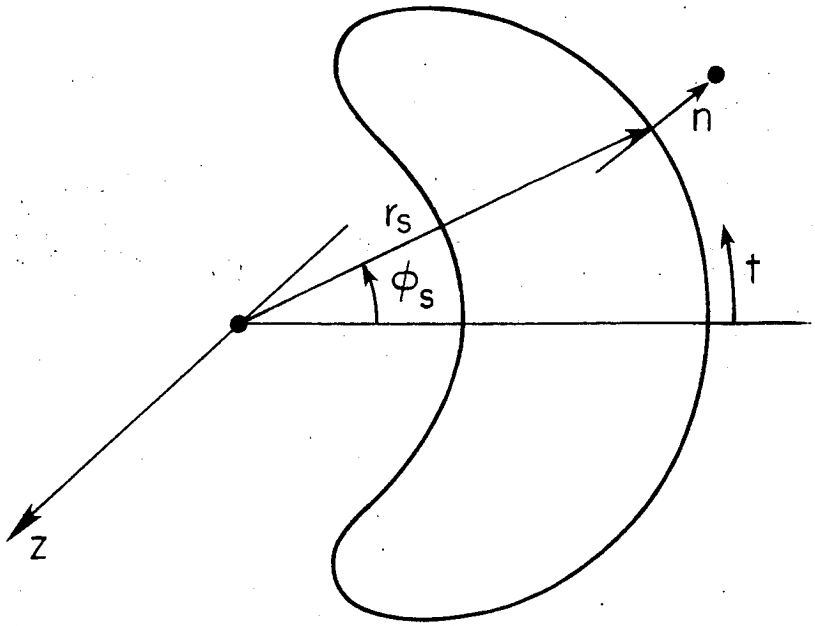

Fig. 1

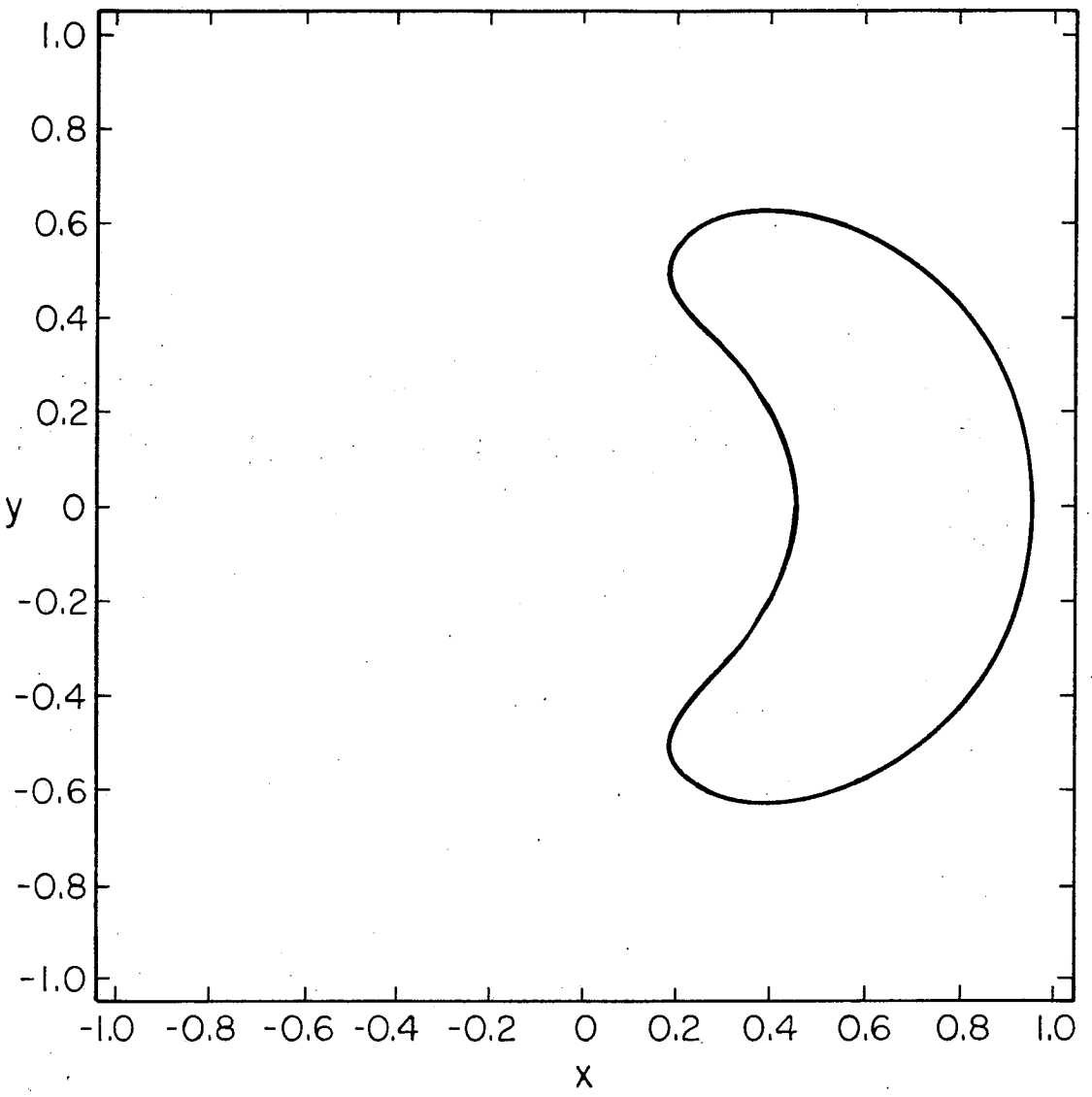

Fig. 2

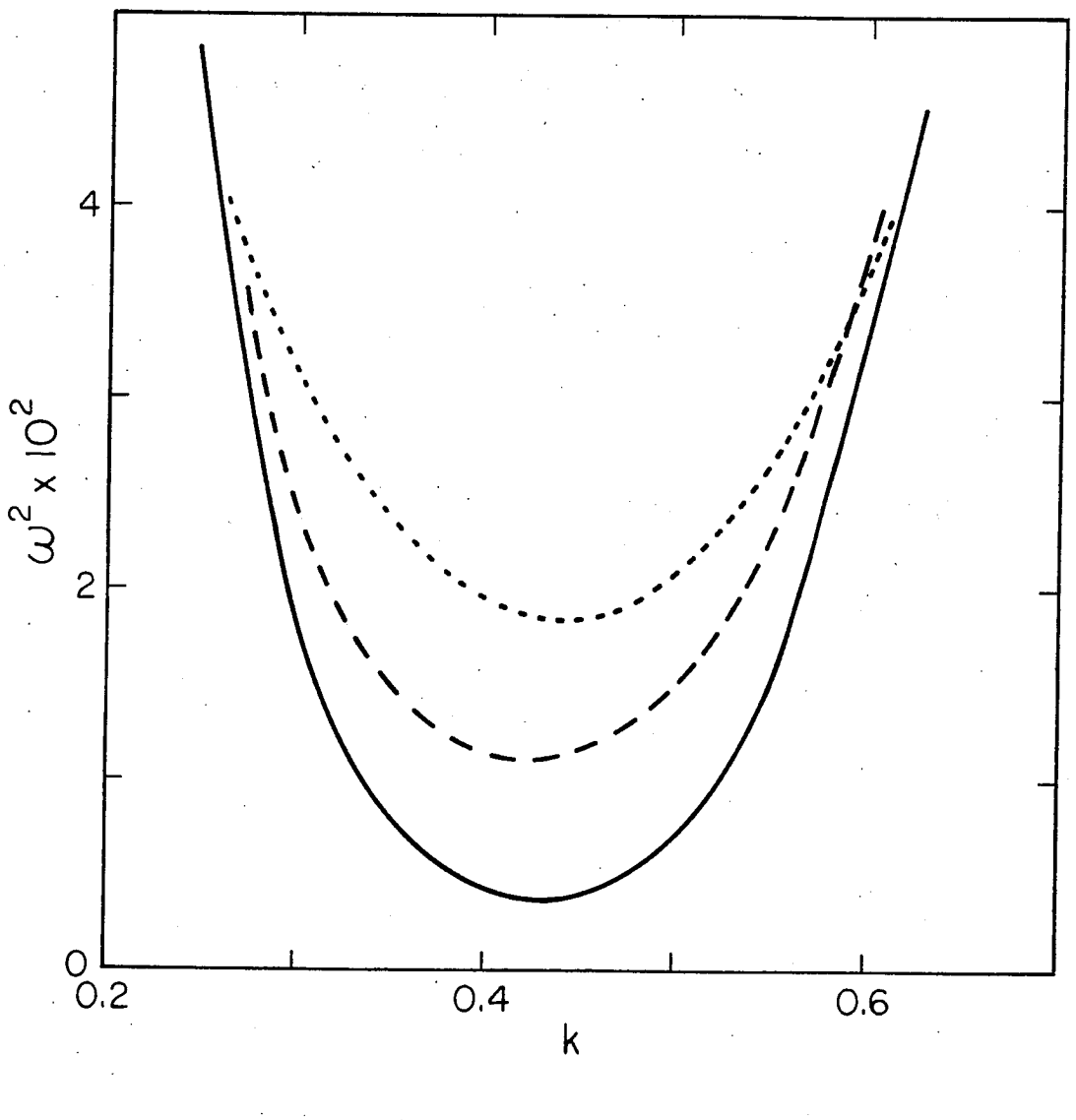

Fig. 3

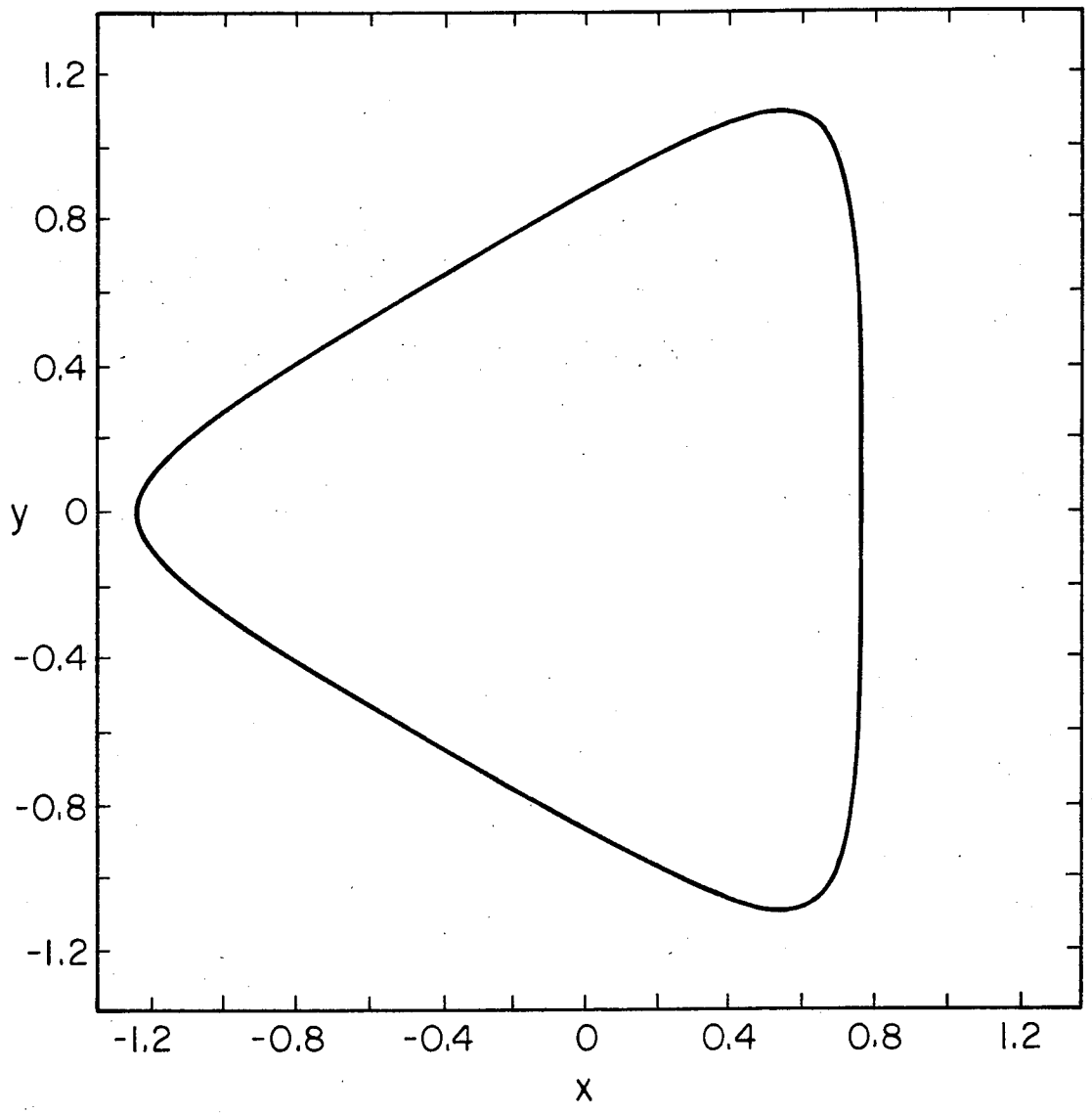

Fig. 4

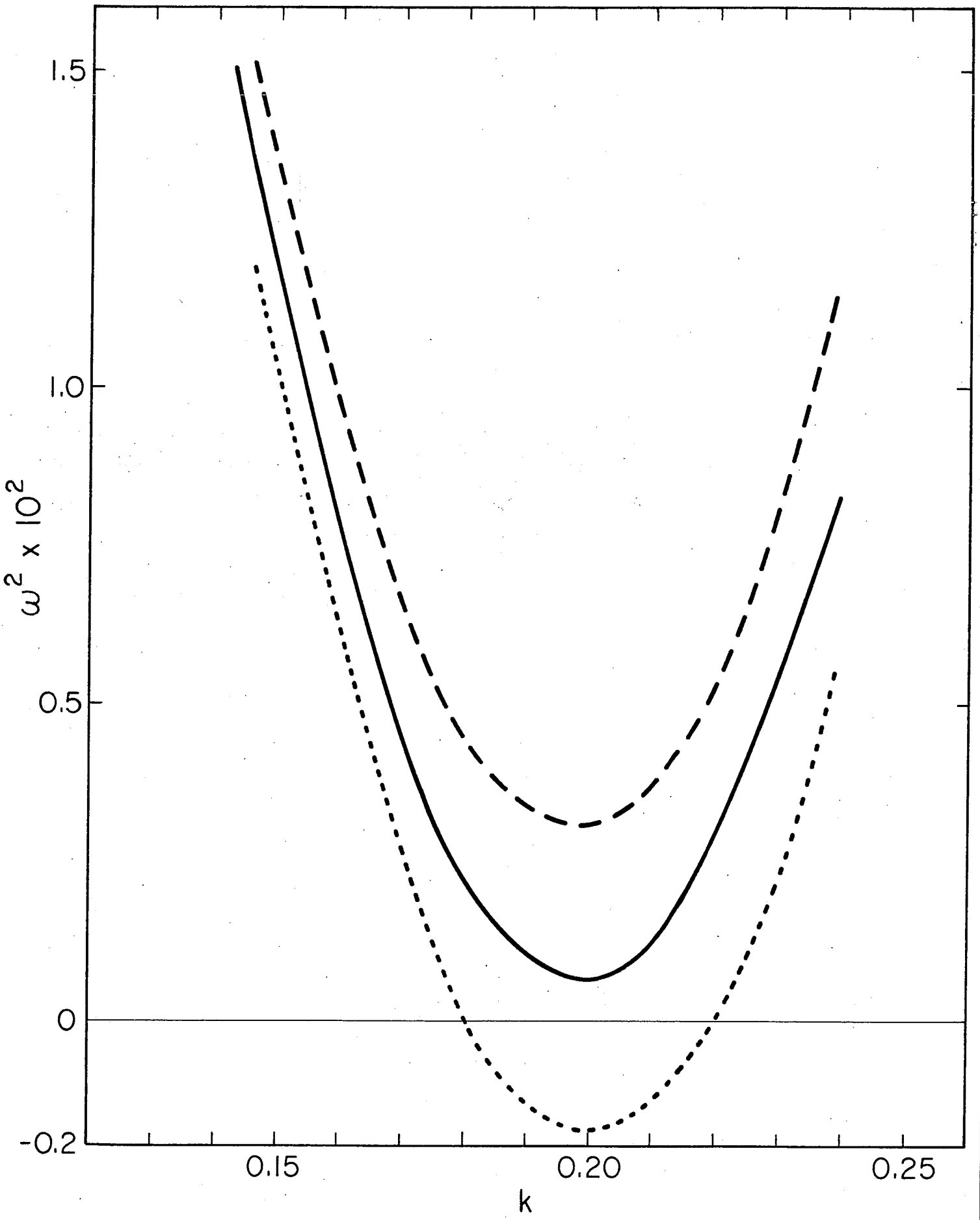

Fig. 5

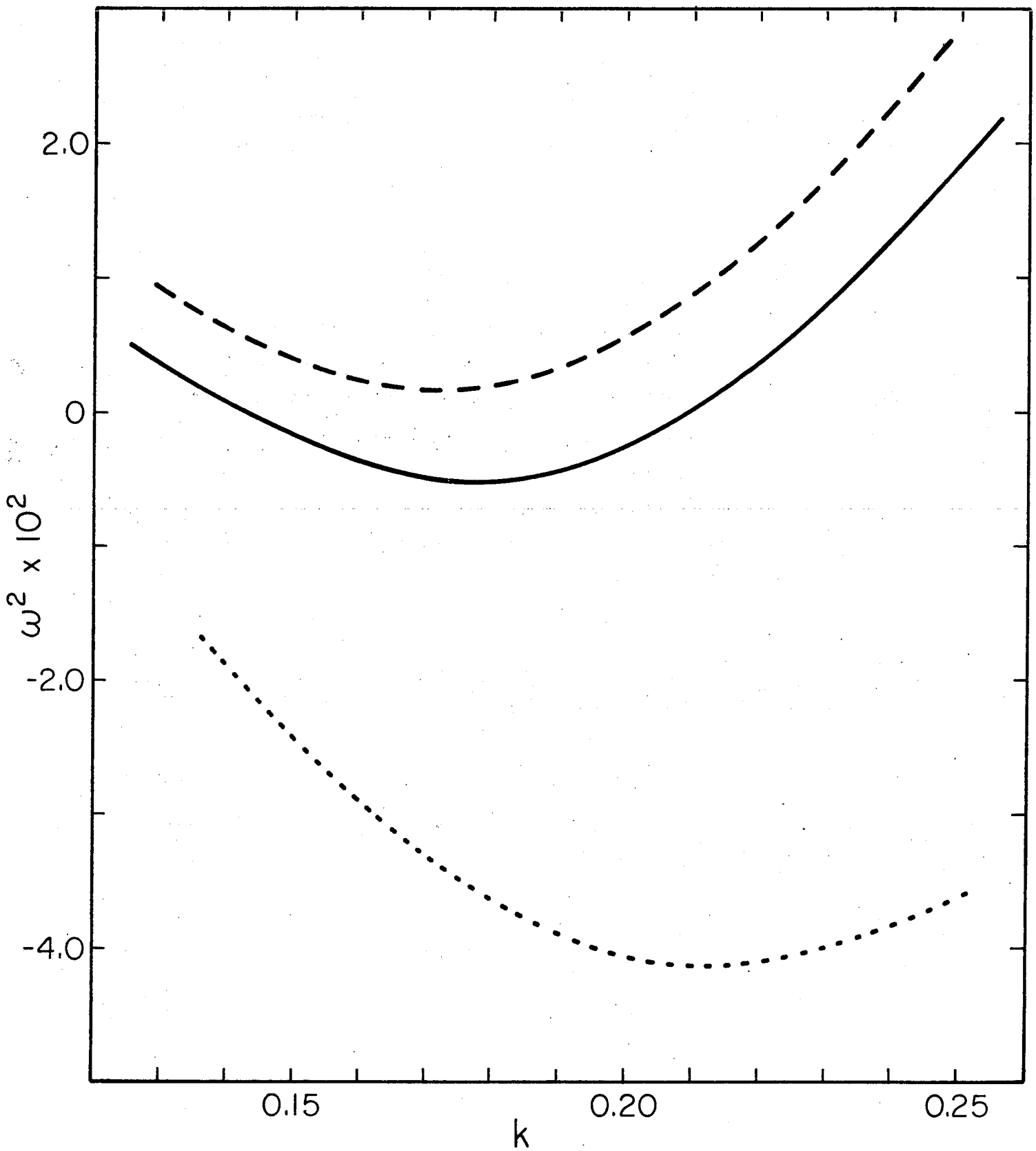

Fig. 6